Pharmaceutical Research, Vol. 25, No. 2, February 2008 (© 2007)
DOI: 10.1007/s11095-007-9467-1

Research Paper

An Investigation into the Dispersion Mechanisms of Ternary Dry Powder Inhaler Formulations by the Quantification of Interparticulate Forces

Matthew D. Jones,[1,3] Jennifer C. Hooton,[1,4] Michelle L. Dawson,[2] Alan R. Ferrie,[2] and Robert Price[1,5]

Received July 20, 2007; accepted October 1, 2007; published online October 19, 2007

Purpose. To investigate the dispersion mechanism(s) of ternary dry powder inhaler (DPI) formulations by comparison of the interparticulate adhesions and *in vitro* performance of a number of carrier–drug–fines combinations.
Materials and Methods. The relative levels of adhesion and cohesion between a lactose carrier and a number of drugs and fine excipients were quantified using the cohesion–adhesion balance (CAB) approach to atomic force microscopy. The *in vitro* performance of formulations produced using these materials was quantified and the particle size distribution of the aerosol clouds produced from these formulations determined by laser diffraction.
Results. Comparison between CAB ratios and formulation performance suggested that the improvement in performance brought about by the addition of fines to which the drug was more adhesive than cohesive might have been due to the formation of agglomerates of drug and fines particles. This was supported by aerosol cloud particle size data. The mechanism(s) underlying the improved performance of ternary formulations where the drug was more cohesive than adhesive to the fines was unclear.
Conclusions. The performance of ternary DPI formulations might be increased by the preferential formation of drug–fines agglomerates, which might be subject to greater deagglomeration forces during aerosolisation than smaller agglomerates, thus producing better formulation performance.

KEY WORDS: adhesion; agglomeration; atomic force microscope; fines; ternary interactive mixture.

INTRODUCTION

The effects of fine excipient particles ("fines") on the behaviour and performance of carrier-based dry powder inhaler (DPI) formulations are well known and have recently been extensively reviewed (1). In summary, the removal of intrinsic fines from a lactose carrier has been shown to decrease the respirable dose of drug delivered by a formulation, whilst the addition of fines to a formulation, typically with a median diameter of 5–10 μm, has been shown to increase its performance (2,3). Fines of various materials, for example glucose, lactose, mannitol and sorbitol, have been shown to produce this effect (4,5) and it is also known that factors such as the concentration of added fines and their particle size and shape can affect the performance of the formulation (6–8).

Despite all this knowledge, the mechanism by which these effects are produced is unclear. Two mechanisms have been proposed: the "active sites" hypothesis and the "agglomerates" hypothesis (1). The active sites hypothesis proposes that fines preferentially adhere to the most "adhesive" areas of the carrier (the active sites), thus forcing drug particles to adhere to less "adhesive" areas. During aerosolisation and dispersion of the formulation, drug particles are therefore more easily liberated from the surface of the carrier, increasing the amount of drug available for inhalation (1,2,9). The agglomerates hypothesis proposes that fine drug particles and fine excipient particles agglomerate with each other in the formulation, forming structures that are more easily removed from the carrier surface during aerosolisation and dispersion than single drug particles, due to their greater detachment mass (1,6,10). Such a phenomenon might increase the amount of drug aerosolised in particles small enough for inhalation.

There is limited, and occasionally conflicting, evidence in support of both hypotheses, but it remains inconclusive (1). Further investigations into this vexed question are, therefore, desirable, as a greater understanding of the dispersion

[1] Pharmaceutical Surface Science Research Group, Department of Pharmacy and Pharmacology, University of Bath, Bath, BA2 7AY, UK.
[2] GlaxoSmithKline Research and Development, Park Road, Ware, Herts, SG12 0DP, UK.
[3] *Present address*: Department of Pharmaceutics, The School of Pharmacy, University of London, 29/39 Brunswick Square, London, WC1N 1AX, UK.
[4] *Present address*: AstraZeneca R&D, Silk Road Business Park, Charter Way, Macclesfield, Cheshire, SK10 2NA, UK.
[5] To whom correspondence should be addressed. (e-mail: r.price@bath.ac.uk)

ABBREVIATIONS: AFM, Atomic force microscopy; CAB, Cohesion–adhesion balance; CV, Coefficient of variation; DPI, Dry powder inhaler; ED, Emitted dose; FFD, Formoterol fumarate dihydrate; FP, Fluticasone propionate; FPD, Fine particle dose; FPF, Fine particle fraction; GSD, Geometric standard deviation; HPLC, High performance liquid chromatography; MMAD, Mass median aerodynamic diameter; NGI, Next Generation Impactor; R_a, Mean roughness; R_q, Root mean square roughness; SEM, Scanning electron microscope; SX, Salmeterol xinafoate.

mechanisms at work within such ternary DPI formulations might be a valuable aid to the rational selection of a fine excipient with the physicochemical characteristics most likely to yield optimal performance.

Both proposed mechanisms hinge on the extent to which a certain type of interparticulate adhesion dominates the behaviour of the formulation: fines–carrier adhesion under the active sites hypothesis and drug–fines adhesion under the agglomerates hypothesis. Examination of interparticulate adhesions within ternary DPI formulations might, therefore, be fruitful. To date, this has only received limited investigation (1,5,7). The aim of this study, therefore, was to further investigate the dispersion mechanism(s) of ternary DPI formulations by comparison of the interparticulate adhesions and *in vitro* performance of a number of carrier–drug–fines combinations. It was hypothesised that if the type of interparticulate adhesion dominating formulation performance could be determined, the mechanism by which fines exert their effects might be further elucidated.

Recently, a novel approach to the quantification of interparticulate forces by colloidal probe atomic force microscopy (AFM) has been developed (11). Known as the cohesive–adhesive balance (CAB) approach, this techniques enables the measurement of the ratio between the cohesion of one material and its adhesion to another material for an equivalent contact geometry, thus overcoming the problems incurred by the unknown contact area between an AFM colloidal probe and substrate (12). A limitation of the technique is its use of highly crystalline substrates of controlled geometry. In contrast, the particles found in actual formulations contain amorphous surface regions and show variable surface morphology. These differences could have a large effect on interparticulate forces and therefore pose a challenge in relating CAB ratios to the behaviour of formulations. However, the CAB technique has proved to be a powerful tool for investigating the behaviour and performance of a number of types of DPI formulation (13–15), as it is important to understand fundamental interparticulate interactions before moving on to consider those found between the heterogeneous particles of an actual formulation. The CAB technique was therefore selected for use in this study, with due regard to its limitations employed during data interpretation. By using a lactose carrier, four drugs and four fine excipients, a total of 16 different ternary formulations were investigated. The CAB approach was employed to quantify the relative levels of cohesion and adhesion present in these formulations, which were then compared to their *in vitro* performance.

MATERIALS AND METHODS

Materials

Micronised fluticasone propionate (FP) and salmeterol xinafoate (SX) were donated by GlaxoSmithKline Research and Development (Ware, UK). Micronised budesonide and formoterol fumarate dihydrate (FFD) were used as supplied. Erythritol was donated by Cerestar (Castelmassa (Ro), Italy), D-mannitol (β-form) was obtained from Sigma-Aldrich (Gillingham, UK) and α,α-trehalose dihydrate was donated by British Sugar (Peterborough, UK). Milled α-lactose monohydrate (*Sorbolac 400*) was obtained from Meggle GmbH (Wasserburg, Germany) and coarse carrier α-lactose monohydrate (*Lactohale*) was donated by Friesland Foods Domo—Pharma (Zwolle, The Netherlands). These excipients will be referred to as erythritol, lactose, mannitol and trehalose. All solvents were supplied by Fisher Scientific UK (Loughborough, UK) and were of at least analytical grade. Water was prepared by reverse osmosis (MilliQ, Molsheim, France).

Methods

Temperature Controlled Dissolution of Carrier Lactose

The design of this study required that only the fines deliberately added to a formulation were active in improving its performance. The proportion of intrinsic fines in the carrier lactose was therefore reduced using a temperature controlled dissolution process (16). The as-received carrier lactose (*Lactohale*) was sieved to obtain the 63–90 μm size fraction using stainless steel sieves (Endecotts Limited, London, UK) and an Analysette 3 PRO vibratory sieve shaker (Fritsch GmbH, Idar-Oberstein, Germany) set to an amplitude of 0.8 mm. Ten percent of the initial mass of this size fraction was then dissolved following a method described elsewhere (16). Finally, the treated material was sieved again to obtain the 63–90 μm size fraction.

Micronisation to Produce Fine Excipients

Erythritol, milled lactose, mannitol and trehalose were micronised using an ultracentrifuge mill (model ZM 100, Retsch GmbH and Co. KG, Haan, Germany) cooled with dry ice and perfused with dry nitrogen. By varying the configuration of the mill, it was possible to produce four fine excipients with reasonably similar particle size distributions and a median particle diameter in the range 5–10 μm (the size of fines that produces the greatest increase in DPI performance (1)).

Particle Size Analysis

Particle size analysis was carried out in the dry state. Powders were dispersed with compressed air at 3 bar through a RODOS dry disperser fed by an ASPIROS micro-dosing unit before sizing with a HELOS laser diffraction sensor (all from Sympatec GmbH, Clausthal-Zellerfeld Germany). Particle size analysis was performed using WINDOX 4.0 software (Sympatec GmbH, Clausthal-Zellerfeld Germany). Particle size summary statistics are the average of three determinations.

Quantification of Cohesion–Adhesion Balances

Two sets of CAB ratios were quantified: drug–fines and fines–carrier. Drug–fines CAB ratios were measured with drug particle colloidal probes and describe the cohesion of drug probes to a drug substrate crystal, relative to the adhesion of the same drug probes to an excipient substrate crystal. Fines–carrier CAB ratios were measured with fine excipient colloidal probes and describe the cohesion of fine excipient probes to an

excipient crystal, relative to the adhesion of the same fine excipient probes to a lactose substrate crystal. The lactose fines–carrier CAB ratio was not quantified, as the cohesion and adhesion measurements would have been identical, thus automatically yielding a ratio of 1.00.

Controlled crystallisation of substrate surfaces. The CAB procedure requires the use of extremely smooth single crystals as substrates for cohesion and adhesion measurements. Such substrates for all the study materials were therefore nucleated and grown on glass cover slips, using techniques described elsewhere (11, 15). The surface topography of the resultant crystals was investigated with TappingMode™ AFM using a Multimode AFM, J-type scanner, Nanoscope IIIa controller (all from DI, Cambridge, UK) and a silicon tip (model number OMCL-AC240TS, Olympus, Japan) to image 10 μm×10 μm square areas of the crystal surfaces with a resolution of 512×512 pixels and a scan rate of 1 Hz. The roughness of imaged areas was quantified using the mean (R_a) and root mean square (R_q) of the variations in the height of the imaged surface, as calculated by the AFM software. To enable identification of the Miller index of the dominant growth face of each crystalline substrate, literature data on the unit cell lattice parameters and space group symmetry operators of the study materials (17–24) were used to model their crystal habits with a 3D crystal simulation program (SHAPE v. 7.0 professional edition, Shape Software, Tennessee, USA).

AFM colloidal probe preparation. Three colloidal probes of each drug and each fine excipient (excluding lactose) were prepared following the method described in detail elsewhere (25). In summary, to prepare a probe, a single particle of micronised material was fixed to the end of a V-shaped tipless cantilever with a nominal spring constant of 0.58 N m^{-1} (Veeco NanoProbe™, model number: NP-OW, Veeco Instruments SAS, Dourdan, France) using an epoxy resin glue (*Araldite Precision*, Bostik Ltd, Leicester, UK) and custom built micromanipulation equipment. The procedure was observed with an optical microscope using a 16× lens. After preparation, the probes were visually inspected using an optical microscope with incident illumination and 50× lens to ensure that a single particle was attached in an appropriate position near the end of the cantilever and that there was not excess glue present. After adhesive force measurements had been completed, this was confirmed by scanning electron microscopy.

Adhesive and cohesive force measurement. The adhesive or cohesive force between each colloidal probe and the dominant face of a smooth crystal of each relevant material was measured with force-volume mode AFM using a Multimode AFM, J-type scanner and Nanoscope IIIa controller (all from DI, Cambridge, UK). 1024 (32×32) individual force curves were collected over a 10 μm×10 μm area of the crystal substrate with a z-scan rate of 4.07 Hz and a nominal compressive loading of 11.6 nN. Humidity within the sample area of the AFM head was maintained at 26°C (±2°C) and 35% RH (±3%), using the method previously described (25).

Force-volume data were processed using custom software to extract the force of adhesion/cohesion from each of the 1,024 force curves. This calculation was performed using the nominal cantilever spring constant of 0.58 N m^{-1} (rather than the measured spring constant of each individual probe) as the comparison of the cohesion and adhesion of the same probe in the CAB method eliminates the effects of cantilever-to-cantilever spring constant variation (15).

In Vitro Formulation Testing

Formulation blending. Binary formulations (i.e. no fines) containing 1.5%$^{w}/_{w}$ drug were prepared in 4 g batches by geometrically mixing the drug and carrier lactose in a 15 ml glass tube for 60 s on a Whirlimixer (Fisons Scientific Equipment, Loughborough, UK). The resultant blend was further mixed using a Turbula shaker-mixer (Willy A Bachofen AG, Basel, Switzerland) at 46 rpm for 40 min.

Ternary formulations (i.e. containing fines) were prepared by first blending the fines and coarse carrier. The initial blends of 10.2%$^{w}/_{w}$ fine excipient and coarse lactose were prepared in 50 g batches in a 100 ml glass bottle following the blending technique employed for the binary formulations. These mixtures were then blended with 1.5%$^{w}/_{w}$ drug in 4 g batches in a 15 ml glass tube using the same blending technique to produce ternary formulations containing 1.5%$^{w}/_{w}$ drug, 10%$^{w}/_{w}$ fines and 88.5%$^{w}/_{w}$ carrier lactose.

Content uniformity determination. Following blending, the drug content uniformity of all the formulations was assessed. Formulations were spread evenly over a clean surface and ten samples of 33±1 mg taken from random positions. Each sample was dissolved in a suitable solvent to 50 ml final volume and drug concentration assessed using a validated high performance liquid chromatography (HPLC) assay. The proportion of drug in each sample was calculated and the content uniformity expressed as the coefficient of variation (CV). The content uniformity of the fines was not determined, as the drug was present at a lower concentration and thus presented a greater challenge in achieving uniformity. Therefore, if the drug was found to be uniform, it is likely that the fines were also.

Capsule filling. Each formulation was manually loaded into size 3 gelatin capsules (donated by Capsugel, Bornem, Belgium). Fill weight was 33±1 mg, giving a nominal dose of 482±15 μg drug per capsule. Following filling, capsules were stored in a sealed desiccator containing a saturated solution of potassium carbonate (providing a relative humidity of 44% (26)) for at least 24 h prior to analysis.

Formulation performance analysis. The performance of each formulation was assessed using a Next Generation Impactor (NGI) with pre-separator. The sample cups were immersed in a 1% solution of silicone oil (Acros Organics, Geel, Belgium) in hexane and allowed to dry before use. A *Rotahaler®* (GlaxoSmithKline, Ware, UK) was attached to the throat of the NGI (Copley Scientific Ltd, Nottingham, UK) using a rubber mouthpiece, a capsule inserted and then opened by twisting the inhaler body. The contents of the capsule were aerosolised into the NGI at a flow rate of 60 l min^{-1} for 4 s. Once the contents of ten capsules had been aerosolised, the equipment was dismantled and the inhaler and capsules, and each part of the NGI, washed down into separate

Table I. Summary Particle Size Statistics of the Study Materials (n=3)

	d_{10} (μm ± SD)	d_{50} (μm ± SD)	d_{90} (μm ± SD)	% <5 μm (± SD)	% <10 μm (± SD)
Micronised budesonide	0.46±0.02	1.44±0.01	3.62±0.03	97.6±0.17	–
Micronised FP	0.51±0.05	1.79±0.13	3.95±0.26	96.7±1.45	–
Micronised FFD	0.64±0.01	1.70±0.00	3.30±0.02	99.2±0.04	–
Micronised SX	0.53±0.01	1.52±0.02	3.54±0.02	97.8±0.06	–
Treated 63–90 μm carrier lactose	49.32±1.07	89.40±0.94	140.15±2.76	–	2.3±0.22
Erythritol fines	1.72±0.03	5.99±0.15	21.27±0.99	–	73.3±1.58
Lactose fines	2.06±0.06	9.35±0.26	24.95±0.78	–	53.2±1.32
Mannitol fines	1.08±0.01	6.99±0.02	21.71±0.54	–	63.5±0.27
Trehalose fines	1.10±0.02	5.41±0.04	16.06±0.20	–	75.6±0.24

known volumes of a suitable solvent. The concentration of drug in each solution was determined by validated HPLC methods, from which the mass of drug deposited on each part of the NGI could be calculated.

Each formulation was tested four times in this way and in order to allow comparison of formulations with different recovered doses, the results were normalised to 100% drug recovery. This enabled the following parameters to be calculated: emitted dose per capsule (ED, mass of drug recovered from all parts of the NGI), fine particle dose per capsule (FPD, the mass of drug recovered from stages 3 and below of the NGI (<4.46 μm (27))) and fine particle fraction (FPF, the FPD expressed as a percentage of the ED). Analysis of variance (ANOVA) was used to compare mean results and where significant differences were detected (p<0.05), these were located using Tukey's Honestly Significant Difference test. The drug mass median aerodynamic diameter (MMAD) and geometric standard deviation (GSD) were calculated from the drug mass deposition on the NGI stages.

Particle Size Analysis of Formulation Aerosol Clouds

The particle size distributions of the aerosol clouds emitted from a *Rotahaler*® by each formulation and by the treated lactose carrier alone were determined using a HELOS laser diffraction sensor and INHALER module (both from Sympatec GmbH, Clausthal-Zellerfeld Germany) (28). The flow rate through the INHALER module was set at 60 l min^{-1} and the mouthpiece of *Rotahaler*® was inserted directly into the measuring chamber, to enable measurement of the particle size distribution of the aerosol cloud immediately after emission. For each measurement, a capsule of formulation was inserted into the *Rotahaler*®, opened by twisting the inhaler body and its contents aerosolised through the laser of the diffraction sensor for 10 s. Particle size analysis was performed using WINDOX 4.0 software (Sympatec GmbH, Clausthal-Zellerfeld Germany). Particle size distributions and values presented are the average of three determinations.

RESULTS AND DISCUSSION

Particle Size Analysis

The particle size distributions of the drugs, treated carrier lactose and micronised fines each approximated to a log-normal distribution, which is usual for such materials. They were, therefore, summarised using the d_{10}, d_{50} and d_{90} values and the proportion of particles smaller than 5 or 10 μm diameter (see Table I). The particle size distributions and summary statistics of the four drugs were very similar, with the vast majority of particles smaller than 5 μm diameter, making them suitable for DPI formulation (29). The success of the dissolution process in reducing the amount of intrinsic fines in the carrier lactose is demonstrated by the low proportion of particles <10 μm diameter it contained (2.3%). The particle size distributions of the micronised fines were essentially similar, as was the aim of the micronisation process. This is reflected by the summary particle size statistics (Table I), which also show that the aim of a median diameter in the range 5–10 μm was achieved.

Quantification of Cohesion–Adhesion Balances

Substrate crystals with a well defined crystal habit and a surface roughness on the dominant face of <1 nm R_a and R_q were successfully grown. These were, therefore, deemed suitable for use in colloidal probe AFM, as their smooth surfaces would enable reproducible adhesion and cohesion measurements (11). Comparison of the habits of these crystals with the appropriate 3D crystal habit simulations enabled the identification of the Miller index of their dominant faces (see Table II). Where a material could crystallise as one of several polymorphs, the probable form obtained was suggested by the crystallisation conditions and the habit of the crystal.

Table II. Probable Polymorph and Dominant Face Miller Index of Extremely Smooth Crystal Substrates used for Colloidal Probe AFM Adhesion and Cohesion Measurements

Material and Polymorph	Dominant Face
Budesonide	{102}
Fluticasone propionate (form I)	{110}
Formoterol fumarate dihydrate	{002}
Salmeterol xinafoate (form I)	{001}
Erythritol	{020} or {200}
α-lactose monohydrate	{100}
D-mannitol (β-polymorph)	{002}
α,α-trehalose dihydrate	{110}

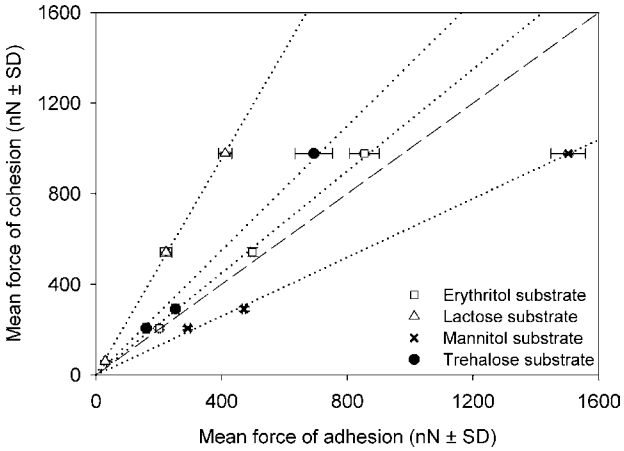

Fig. 1. Representative CAB graph, showing the relationship between the cohesion of SX colloidal probes with the SX crystalline substrate and the adhesion of the SX colloidal probes with the four excipient crystalline substrates. This graph was constructed using five different colloidal probes, as some probes were damaged part-way through the measurement cycle. The *dashed line* shows where cohesion = adhesion.

The adhesive or cohesive force between each colloidal probe and the dominant face of the crystalline substrate of each relevant material was successfully measured. Due to the use of extremely smooth substrates, the distribution of forces obtained for each measurement followed a normal distribution, and were therefore summarised by their mean and standard deviation. In accordance with the CAB procedure, the mean cohesive force for each colloidal probe was plotted against its mean adhesive force to each relevant substrate to produce a CAB graph (Fig. 1) (11). Linear regression analysis through the origin of each set of CAB data showed a high degree of linearity (R^2>0.83 in all cases), confirming that the contact area between colloidal probes and substrates remained constant for both adhesive and cohesive measurements (11). The gradient of each line of best fit was therefore taken as the CAB ratio (Tables III and IV) (11).

Each CAB ratio describes (all other variables being equal) the cohesion of the colloidal probe material relative to its adhesion to the crystalline substrate of the second material (11). A CAB ratio <1 (termed an adhesive CAB ratio), therefore, describes a situation where the adhesion between the two materials is greater than the cohesion of the colloidal probe material. The closer a CAB ratio is to zero, the greater the adhesion is compared to the cohesion. On the other hand, a CAB ratio >1 (termed a cohesive CAB ratio) describes a system where the cohesion of the colloidal probe material is greater than its adhesion to the other material in question. As the relative magnitude of this cohesion increases, so does the CAB ratio. For example, the SX–lactose CAB ratio is 2.39, indicating that, all other variables being equal, the cohesiveness of SX is 2.39 times greater than its adhesiveness to lactose. The FP–lactose CAB ratio is 0.22, however, indicating that, all other variables being equal, the cohesiveness of FP is 0.22 times smaller than its adhesiveness to lactose, or alternatively, the adhesiveness is 4.55 times greater than the cohesiveness.

Budesonide–lactose CAB ratios have previously been measured as 4.54 (11) and 1.19 (30), whereas in this study it was 0.82±0.08. Equally, the budesonide–trehalose CAB ratio was previously measured as 0.82 (30), compared with 1.07±0.06 in this study. Although initially counterintuitive, these measurements were each made with a different batch of micronised budesonide, each of which would have been subject to a different process history producing variable surface properties. Such variation in CAB ratios may, therefore, be attributed to this phenomenon, as discussed elsewhere (15).

In Vitro Formulation Testing

The drug content uniformity measurements of the 20 formulations tested are shown in Table V. As these data show, not all the formulations had a drug CV <6%, which is the value commonly taken as sufficiently uniform for DPI systems. For the purposes of this study, however, it was important that all formulations were blended in a consistent manner, in order to allow the effects of varying CAB ratios to be observed. In addition, a relatively low shear blending procedure was employed to ensure that subtle differences in blend structure caused by varying CAB ratios would not be overcome by putting a large amount of energy into the formulation during mixing. For these reasons, the blending process was not altered to bring the CV of all formulations to <6%.

The *in vitro* drug deposition in the NGI is summarised in Table V. As shown in Fig. 2, the performance of the various formulations, as measured by both FPD and FPF, showed a considerable number of significant differences (ANOVA p<0.001 in all cases). As has previously been shown in many reports (1), in the vast majority of cases, the addition of fines led to a significant increase in formulation performance, although this was not the case for every formulation. For example, the addition of erythritol or trehalose fines did not produce a significant increase in the FPD of budesonide or formoterol fumarate dihydrate, although there was a non-significant increase in FPD for all of these ternary formulations. Although rare, there are reports in the literature

Table III. CAB Ratios (± SD) and Respective Coefficients of Determination (R^2) for the Interactions of Drug Colloidal Probes with Excipient Substrates

CAB Ratio ± SD (R^2)		Colloidal Probe			
		Micronised Budesonide	Micronised FP	Micronised FFD	Micronised SX
Crystalline substrate	Erythritol	0.96±0.02 (0.9989)	0.77±0.05 (0.9202)	1.00±0.05 (0.9640)	1.12±0.02 (0.9965)
	Lactose	0.82±0.08 (0.9315)	0.22±0.00 (0.9932)	1.16±0.11 (0.8683)	2.39±0.02 (0.9995)
	Mannitol	1.12±0.06 (0.9873)	0.46±0.03 (0.9249)	1.18±0.07 (0.9370)	0.65±0.01 (0.9986)
	Trehalose	1.07±0.06 (0.9706)	0.70±0.05 (0.9128)	1.02±0.10 (0.8389)	1.37±0.06 (0.9888)

Table IV. CAB Ratios (± SD) and Respective Coefficients of Determination (R^2) for the Interactions of Excipient Colloidal Probes with the Lactose Substrate

CAB Ratio ± SD (R^2)	Colloidal Probes		
	Micronised Erythritol	Micronised Mannitol	Micronised Trehalose
Lactose crystalline substrate	1.16±0.09 (0.9522)	1.21±0.01 (0.9993)	0.54±0.03 (0.9742)

showing that, depending on the formulation materials and processing methods, the addition of fines to a formulation may not change performance (5,31,32), so these findings are not entirely unexpected.

Using the FPD and FPF data, it is possible to draw-up rank orders showing the effects of the various fine materials on the performance of the four different drugs:

Budesonide: Lactose > Mannitol > Erythritol > Trehalose
FP: Mannitol > Lactose > Trehalose > Erythritol
FFD: Lactose > Mannitol > Trehalose > Erythritol
SX: Mannitol > Trehalose > Lactose > Erythritol

The rank order for each of the four drugs is different, suggesting that the varying effects of the different fines are not attributable to one or other of their intrinsic properties, for example, their particle size distributions or shapes. Rather, these data suggest that their varying effects are attributable to a property that varies depending upon the drug with which they are formulated, such as the magnitude of the adhesion between the drug and fines particles.

The Relationships between Formulation CAB Ratios and Performance

As discussed, the aim of this study was to compare the performance of ternary formulations with their interparticulate interactions, in an attempt to further elucidate the mechanism(s) responsible for the effects of fines. Inspection of Fig. 2 reveals, however, that the performance of the four drugs varied considerably, with, for example, FP formulations producing considerably poorer performance than FFD formulations. This can be attributed to the varying physicochemical properties of each drug giving it an intrinsic level of performance. One of the most important factors in controlling drug intrinsic performance may have been its CAB ratio with the carrier, as this varied from 0.22 for the FP–lactose interaction to 2.39 for the SX–lactose interaction (see Table III), which has previously been shown to have a dramatic effect on formulation performance (15,30).

Given this phenomenon, any attempt to pool the performance data for formulations of the four drugs and compare them to CAB ratios would be unlikely to succeed, as the differences in the intrinsic performance of the drugs would outweigh variations in formulation performance attributable to differing interactions between the various types of particle. Ternary formulation FPD was therefore normalised, by division by the FPD of the respective binary formulation. Thus, the variation in the intrinsic performance of the four drugs was cancelled out, with the resultant data showing the relative improvement in performance brought about by the addition of fines to the formulation.

Fines–Carrier CAB Ratios

As discussed, if the addition of fines to a formulation improves performance via the hypothetical active sites mech-

Table V. Formulation Content Uniformity and *In Vitro* Performance Parameters from Aerosolisation into the NGI (n=4)

Formulation	Content Uniformity (CV, %)	Mean ED (μg ± SD)	Mean FPD (μg ± SD)	Mean FPF (% ± SD)	MMAD (μm ± GSD)
Budesonide binary	5.67%	290.5±9.7	18.6±3.3	6.4±1.1	4.4±1.8
Budesonide erythritol fines	4.77%	281.7±23.4	22.0±1.2	7.8±0.5	5.5±2.2
Budesonide lactose fines	6.92%	273.8±11.5	34.5±3.7	12.6±1.4	4.6±2.1
Budesonide mannitol fines	6.74%	288.3±3.2	31.6±2.8	11.0±1.0	4.7±2.1
Budesonide trehalose fines	9.35%	288.9±21.7	20.5±1.9	7.1±0.3	5.3±2.1
FP binary	4.90%	349.9±14.2	6.7±0.7	1.9±0.2	4.7±2.1
FP erythritol fines	5.62%	303.7±19.4	11.9±1.5	3.9±0.3	7.2±2.2
FP lactose fines	6.10%	302.9±15.3	20.1±2.4	6.6±0.7	5.6±2.1
FP mannitol fines	3.85%	308.7±24.2	22.4±3.4	7.2±0.8	4.9±2.0
FP trehalose fines	4.44%	310.4±15.5	18.3±1.8	5.9±0.7	5.3±2.1
FFD binary	5.17%	332.7±17.5	15.6±2.1	4.7±0.5	3.3±2.0
FFD erythritol fines	7.69%	297.7±19.3	16.1±1.5	5.4±0.6	6.8±2.4
FFD lactose fines	7.83%	295.9±23.4	36.5±6.6	12.3±1.4	3.9±2.1
FFD mannitol fines	2.90%	285.8±27.0	25.6±2.1	9.0±0.6	4.3±2.1
FFD trehalose fines	10.22%	299.5±19.6	21.9±3.8	7.3±1.4	4.9±2.1
SX binary	4.77%	361.1±9.0	12.3±1.0	3.4±0.2	4.0±2.5
SX erythritol fines	5.10%	325.2±15.1	26.0±6.8	7.9±1.7	5.5±2.5
SX lactose fines	6.58%	330.6±8.0	28.2±2.6	8.5±0.8	4.6±2.3
SX mannitol fines	3.74%	322.8±23.6	36.8±6.4	11.4±1.8	3.8±2.3
SX trehalose fines	1.57%	327.2±18.6	28.2±7.7	8.6±2.0	4.8±2.3

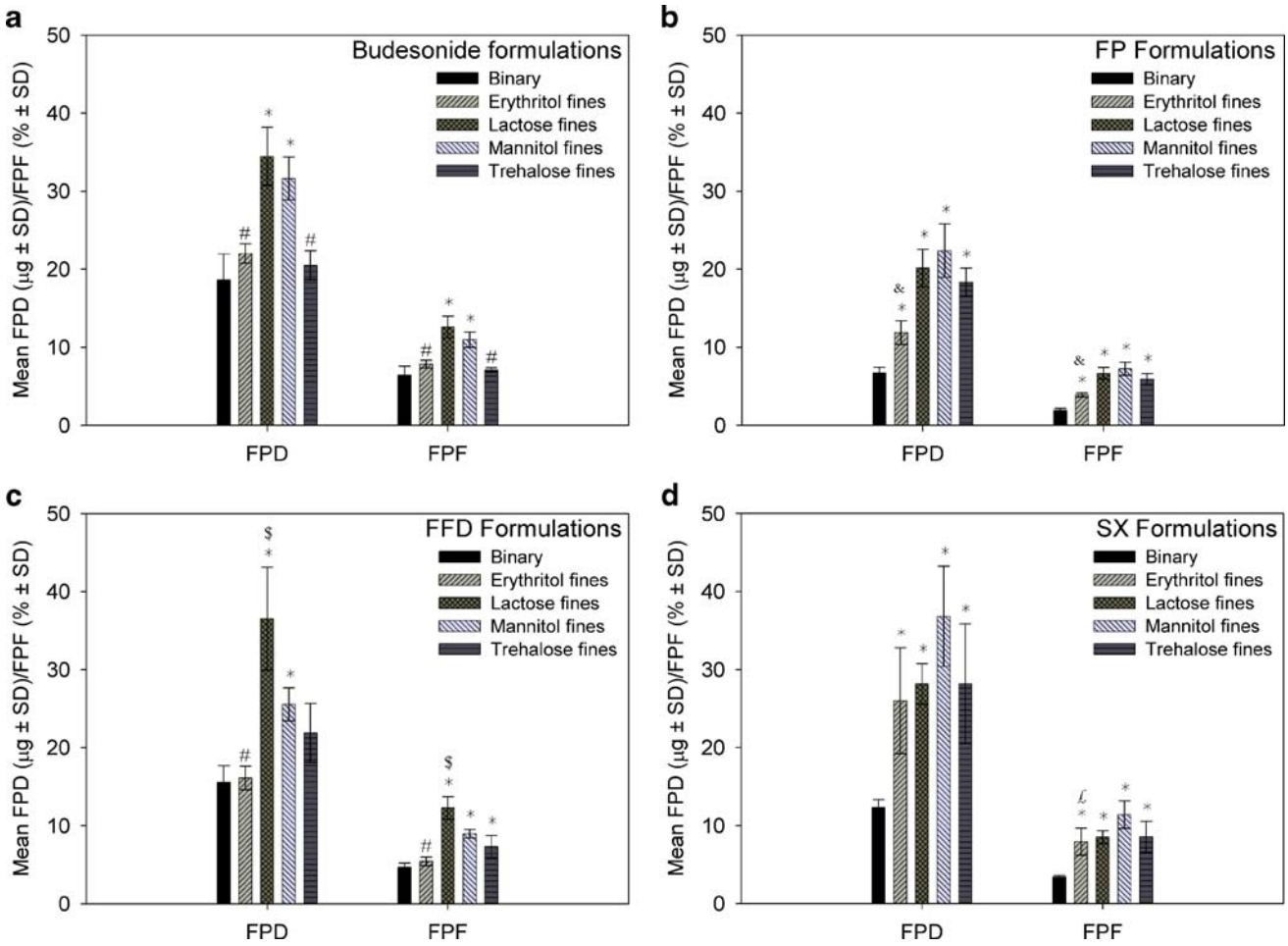

Fig. 2. FPD per capsule and FPF of each formulation (n=4). * = significantly > binary formulation; £ = significantly < mannitol ternary formulation; # = significantly < lactose and mannitol ternary formulations; & = significantly < lactose, mannitol and trehalose ternary formulations; $ = significantly > mannitol and trehalose ternary formulations.

anism, fines–carrier adhesion can be expected to dominate formulation performance. This comparison was therefore made in Fig. 3, by plotting the normalised FPDs of the ternary formulations against their respective fines–carrier CAB ratios (Table IV). If the active sites mechanism were at work, fines that were more adhesive to the carrier (i.e. those with a smaller fines–carrier CAB ratio) would be expected to produce larger increases in formulation performance than less adhesive fines. As no such relationship is evident in Fig. 3, it is possible that this mechanism may not have been responsible for the improved performance of the ternary formulations examined in this study.

Analysis of Fig. 3 is limited by three factors. Firstly, the use of only four materials as fines produced only four fines–carrier CAB ratios to compare with formulation performance. Secondly and as discussed above, the lactose fines–lactose carrier CAB ratio is not a measured value, as both the cohesive and adhesive measurements that would be needed to measure it are the same. It was, therefore, set at 1.00 in Fig. 3. In reality, the adhesion of a micronised lactose particle to a larger lactose carrier particle would be unlikely to have a CAB ratio of 1.00, due to the differing physicochemical properties of these two materials caused by their different process history. Unfortunately, it is not possible to measure the actual ratio using the current CAB approach. Finally, as discussed in the Introduction, the fines–carrier CAB ratios were measured against a highly crystalline, extremely smooth lactose substrate. This surface is unlikely to have contained any active sites, as these are thought to be areas of amorphous material or variable surface morphology (29). The measured fines–carrier CAB ratios may not, therefore, reflect the effects of active sites.

Drug–Fines CAB Ratios

If the addition of fines to a formulation improves its performance via the hypothetical agglomerates mechanism, drug–fines adhesion can be expected to dominate formulation performance. This comparison was therefore made in Fig. 4, by plotting the normalised FPDs of the ternary formulations against their respective drug–fines CAB ratios (Table III).

Inspection of Fig. 4 reveals that there is a relationship between these two sets of data. When the CAB ratio was <1.0 (i.e. drug–fines adhesion was stronger than drug–drug cohesion), decreasing CAB ratio was associated with an increasing normalised FPD. These data suggest that an optimum point was reached, after which normalised FPD decreased, but as there was only one CAB ratio <0.4 and given the error associated with the data, this is unlikely to be statistically significant.

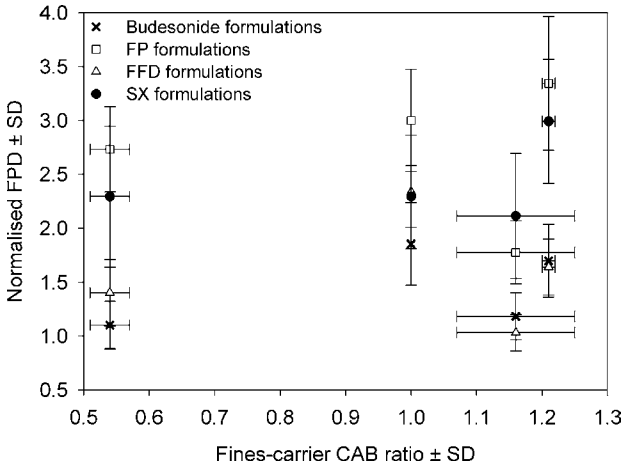

Fig. 3. The relationship between ternary formulation normalised FPD and fines–carrier CAB ratio.

Inspection of Fig. 4 where the CAB ratio was >1.0 (i.e. drug–fines adhesion was weaker than drug–drug cohesion) suggests that there was an initial increase in normalised FPD with increasing CAB ratio. After a CAB ratio of ~1.1 was reached, no further change in normalised FPD was seen, despite a greater than twofold increase in CAB ratio.

The trend of increasing normalised FPD with decreasing adhesive CAB ratio was tested using linear regression. When all the data were included, this yielded a highly significant (p=0.001) R^2 of 0.796. Given the possibility (discussed above) that this trend reaches an optimum, this analysis was repeated excluding the data relating to the FP–lactose fines formulation, which may fall on the opposite side of the maximum to the rest of the data. Once more, this yielded a highly significant (p<0.001) R^2 of 0.913.

These data suggest, therefore, that when the drug particles were more adhesive to the fines than cohesive, increasing relative drug–fines adhesion was associated with greater increases in ternary formulation performance. However, when the drug particles were more cohesive than adhesive to the fines, ternary formulation performance increases were constant and independent of the relative strength of the drug–fines adhesion.

The Mechanism(s) Responsible for the Effects of Fines—Adhesive Drug–fines CAB Ratios

The formation of agglomerates of drug and fines particles is one of the mechanisms proposed for the effects of fines, as it is thought that the greater mass of an agglomerate will enable it to be more easily detached from the surface of a carrier particle than a single drug particle that might be found in a binary formulation (10). The findings of this study support this hypothesis, as for adhesive drug–fines CAB ratios, increasing relative drug–fines adhesion (which might increase the extent of drug–fines agglomeration) is associated with increased ternary formulation performance.

By applying the findings of work recently carried out using simpler DPI formulations, however, it can be demonstrated that stronger drug–fines adhesion, giving rise to larger drug–fines agglomerates, might produce better ternary formulation performance, whatever the effect of particle size on detachment from the carrier. This explanation is speculative and is provided in order to suggest a direction for future research. It is based on work, carried out with drug-only and binary drug–lactose fines formulations, which showed that greater drug cohesion, as demonstrated by a higher CAB ratio, was associated with better *in vitro* performance (13). This was explained by consideration of the drag force (F_{drag}) acting on an agglomerate of drug suspended in an air flow, which can be described by the following equation (13):

$$F_{drag} = C_d \frac{\pi}{8} \rho_a \Phi_{agg}^2 V^2 \quad (1)$$

where C_d is the drag coefficient, ρ_a is the density of air, Φ_{agg} is the effective diameter of the agglomerate and V is the velocity of the air flow. The kinetic energy (E_k) of the agglomerate moving in the air stream is described by (13):

$$E_k = \frac{\pi}{12} \rho_{agg} \Phi_{agg}^3 v^2 \quad (2)$$

where ρ_{agg} is the density of the agglomerate. Therefore, the drag force, which acts to break up the agglomerate, and its kinetic energy, to which the efficiency of deagglomeration by collision is related, increase in proportion to the square and the cube of its diameter. Larger agglomerates will, therefore, be subjected to much greater deagglomeration forces than smaller ones. It was proposed for simple binary DPI formulations that the more cohesive drug produced better *in vitro* performance because although its agglomerates were held together by stronger forces, they also had a larger diameter than those of the less cohesive drug, and so were subject to greater deagglomeration forces (13). It was further proposed that as deagglomeration proceeded, agglomerate size would have reduced, resulting in decreased deagglomeration forces. Eventually, these forces would have been weaker than the internal forces of cohesion holding the agglomerates together, at which point deagglomeration would have ceased, resulting in the formation of metastable agglomerates (13).

As Fig. 5 shows, this theory can be applied to ternary formulations. It is reasonable to assume that a smaller CAB

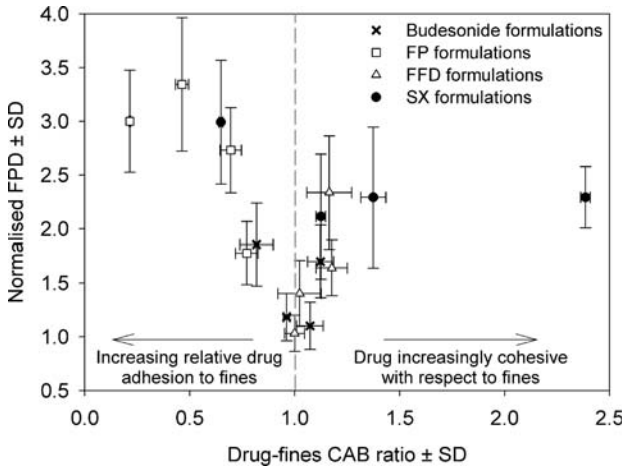

Fig. 4. The relationship between ternary formulation normalised FPD and drug–fines CAB ratio.

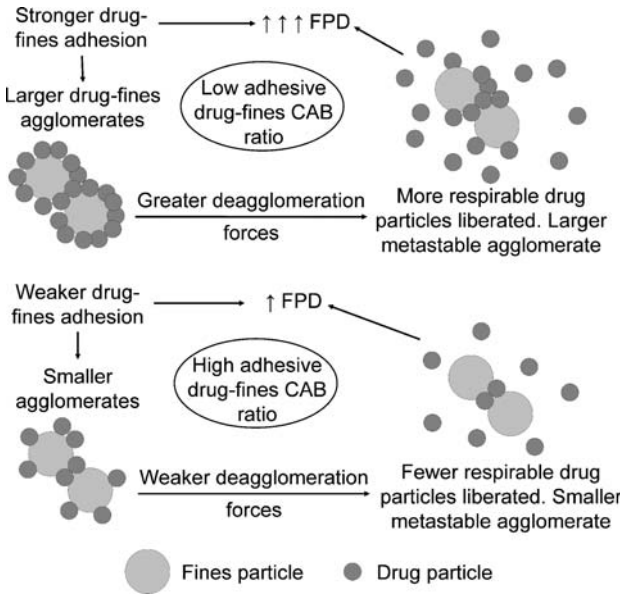

Fig. 5. Schematic of proposed mechanism to explain why lower adhesive drug–fines CAB ratios were associated with better *in vitro* performance than higher adhesive drug–fines CAB ratios.

ratio (i.e. stronger relative drug–fines adhesion) might result in the formation of larger agglomerates of drug and fines particles in a ternary formulation. Such agglomerates might be subjected to greater deagglomeration forces, as described by Eqs. 1 and 2 and thus potentially release more inhalable drug particles than smaller agglomerates, producing better *in vitro* performance.

The Mechanism(s) Responsible for the Effects of Fines—Cohesive Drug–Fines CAB Ratios

So far, only the mechanism at work in formulations with a drug–fines CAB ratio <1 has been considered. When this CAB ratio was >1, ternary formulation performance was found to be independent of the relative strength of the drug–fines adhesion. This suggests that the improved performance of these formulations was not brought about by the formation of agglomerates of drug and fines particles. This is unsurprising, as a cohesive drug–fines CAB ratio indicates that drug particles have a tendency to interact cohesively with other drug particles rather than to interact adhesively with fines particles (11,13). In the absence of significant drug–fines interaction, the strength of the adhesion between drug and fines particles would not be expected to relate to ternary formulation performance.

Some other mechanism must, therefore, be responsible for the improved performance of these formulations. This mechanism may be the passivation of carrier surface active sites, which has been previously proposed by several workers (2,9,33), although as discussed above, the data presented here do not support this hypothesis.

The improvement in the performance of the cohesive formulations was independent of all interparticulate interactions and did not vary significantly between formulations made with different drugs or fines. This suggests that the mechanism responsible for this improvement is related simply to the presence of additional fine particles in the formulation and possibly not to their physical or chemical properties. One possible mechanism which fits this description is particle–particle collision. Numerous studies have shown that the detachment of particles from a stationary surface exposed to an air flow can be greatly increased (by as many as two orders of magnitude) by the collision of particles suspended in the air stream with those adhered to the surface (34–41). A colliding particle can possess up to 1,000 times the momentum of the equivalent volume of air and so provides the adhered particle with more energy to overcome its adhesion to the surface, leading to resuspension into the air stream (34,38,39). This has been shown to be the dominant mechanism responsible for the resuspension of particles in the respirable size range from surfaces (36,41).

Due to their increased proportion of fine particles, ternary formulations contain more particles per unit mass than binary formulations. For example, it is estimated that the ternary formulations used in this study contained greater than 400% more individual particles than the binary formulations. This massive increase in particle number might result in more collisions between particles upon the aerosolisation of a ternary formulation. Given the efficiency with which collision increases particle resuspension from a stationary surface, it is possible that a greater number of collisions during the aerosolisation of a ternary formulation might result in greater drug particle detachment from the carrier and hence improved performance. Once again, this hypothesis is speculative and it is provided to suggest a direction for future research.

Particle Size Analysis of Formulation Aerosol Clouds

The agglomerate formation mechanism for the effects of fines proposed in Fig. 5 suggests that the size of drug–fines agglomerates might be controlled, at least in part, by the strength of the adhesion between drug and fines particles. This proposal was further investigated by examination of the particle size distributions of the aerosol clouds emitted from a *Rotahaler*® by each formulation at the same flow rate (and thus pressure difference over the inhaler) as that employed during NGI testing.

Figure 6 shows the particle size distributions of the aerosol clouds produced by the treated lactose carrier alone,

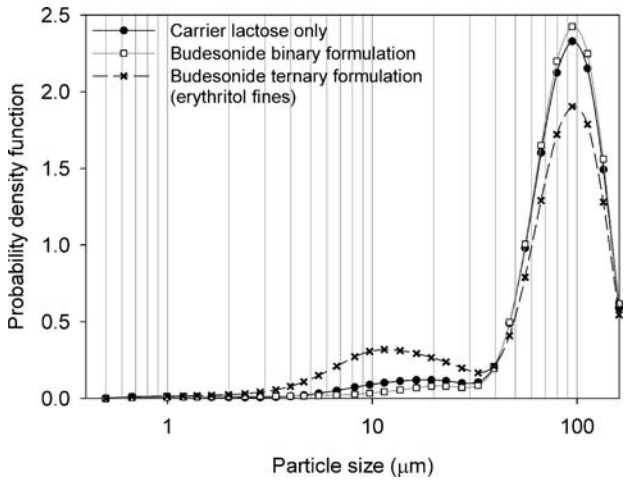

Fig. 6. Representative particle size distributions of the aerosol clouds produced by the various types of formulation tested.

the budesonide binary formulation and the ternary budesonide formulation containing erythritol fines. As these representative data show, all formulation particle size distributions had a mode diameter of ~100 μm, which, by comparison with the particle size distribution of the lactose carrier alone can be attributed to the carrier lactose.

As represented in Fig. 6, the carrier lactose alone and the binary formulations of the four drugs each produced an aerosol cloud with a monomodal particle size distribution with a negative skew, reflecting intrinsic lactose fines and/or drug particles. The 16 ternary formulations, however, produced aerosol clouds with bimodal particle distributions (Figs. 6 and 7). These had a primary mode at ~100 μm (attributable to the lactose carrier) and a secondary mode between 9 and 17 μm.

Given the absence of this secondary mode in the particle size distributions of the aerosol clouds produced by the carrier alone and the binary formulations, it clearly cannot be attributed to intrinsic fines or drug particles. It must, therefore, be related to the presence of fines in the formulations. The particle size at which it occurs is, however, larger than the d_{50} of the fines alone (see Table I) and the position of the secondary mode related to each type of fines varied depending on the drug with which they were formulated (Table VI), so it cannot be attributed to single fines particles either. The secondary mode can, therefore, be attributed to agglomerates of smaller particles, either the drug, the fines or both.

In order to further investigate this phenomenon, the secondary mode particle size was determined from the particle size distributions of the aerosol clouds produced by all the ternary formulations. These data are shown in Table VI. To investigate the proposal that the size of drug–fines agglomerates in a ternary formulation might be related to the strength of the drug–fines adhesion, these secondary mode particle sizes were plotted against the relevant drug–fines CAB ratios (Fig. 8).

As Fig. 8 shows, linear regression analysis found a significant relationship between decreasing adhesive drug–fines CAB ratio (i.e. increasing drug–fines adhesion) and increasing secondary mode particle size. If the secondary mode particle size is taken to reflect the "average" diameter of drug–fines agglomerates within the aerosol cloud, which, as discussed above, is plausible, this finding supports the proposal that increased drug–fines adhesion leads to larger drug–fines agglomerate formation in ternary formulations and, therefore, provides further evidence in support of the mechanism for the action of fines proposed in Fig. 5.

It should be noted that the Fraunhofer laser diffraction approximation used in this work assumes that the particles are spherical (42), which may have produced some inaccuracy in the data. However, this limitation applies equally to all the formulations studied, so comparison of the secondary mode position produced by different ternary mixtures is a valid method of data analysis. It could also be argued that the differences in secondary mode particle size for the adhesive formulations shown in Fig. 8 are attributable to differences in the primary particle size of the fines rather than to the formation of drug–fines agglomerates of varying sizes. Such arguments are undermined, however, by consideration of the relative position of the data relating to formulations containing the same fines. For example, the FP–lactose fines formulation formed the largest secondary mode particle size (16.5±0.2 μm) whilst the budesonide–lactose fines formulation resulted in a much smaller secondary mode particle size (11.8±1.0 μm). Similarly, the FP-erythritol formulation had one of the larger secondary mode particle sizes (14.3±0.7 μm), whilst the same

Table VI. Secondary Mode Particle Size of the Particle Size Distributions of the Aerosol Clouds Produced by the Ternary Formulations (n=3)

	Mean Secondary Mode Particle Size (μm ± SD)			
	Budesonide	FP	FFD	SX
Erythritol fines	12.0±1.3	14.3±0.7	11.7±0.8	11.3±1.2
Lactose fines	11.8±1.0	16.5±0.2	16.0±0.6	14.0±1.7
Mannitol fines	14.0±2.3	15.0±0.3	13.6±2.8	13.2±1.8
Trehalose fines	10.3±0.6	10.5±1.4	9.8±0.4	8.9±0.3

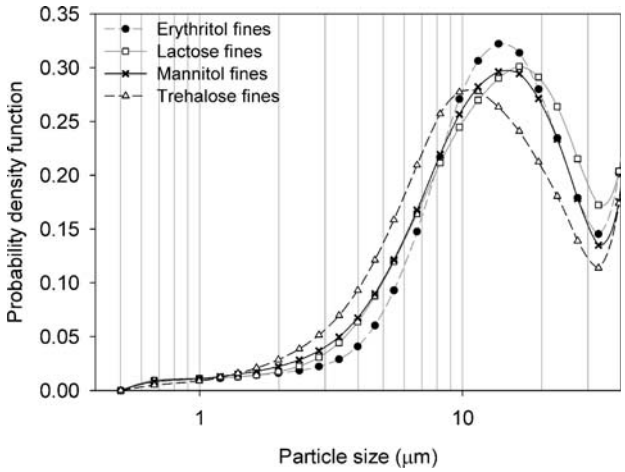

Fig. 7. Expanded view of the secondary mode in the particle size distributions of the aerosol clouds produced by the FP ternary formulations (representative data).

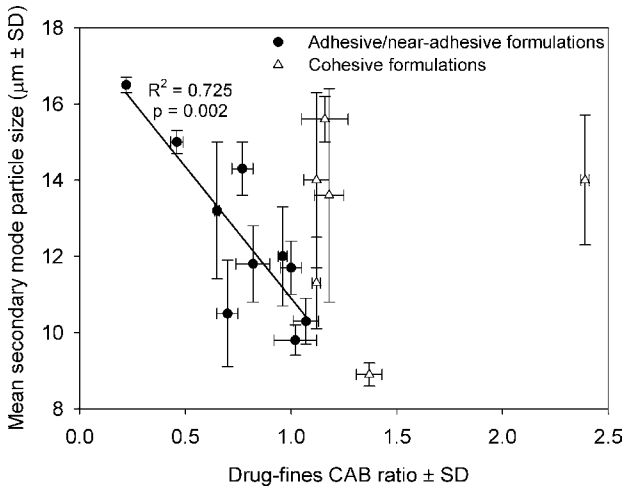

Fig. 8. The relationship between aerosol cloud secondary mode particle size and drug–fines CAB ratio for the ternary formulations.

fines formulated with FFD produced a secondary mode particle size of only 11.7±0.8 μm. Therefore, rather than being dictated by the primary particle size of the fines, the secondary mode particle size seems to be dictated by the relevant drug–fines CAB ratio. Indeed, this CAB ratio is able to overcome, to an extent, the particle size differences of the fines.

As Fig. 8 shows, there was no relationship between secondary mode particle sizes and cohesive drug–fines CAB ratios. This reflects the results presented in Fig. 4, which demonstrate that ternary formulation performance is independent of cohesive drug–fines CAB ratios. These findings are to be expected, because as discussed above, a cohesive drug–fines CAB ratio indicates that the drug and fines particles are unlikely to interact and form agglomerates (11,13).

CONCLUSIONS

The data presented suggest that, in situations where the drug is more adhesive to the fines than cohesive, the improvement in ternary DPI formulation performance brought about by the addition of fines might be due to the preferential formation of agglomerates of drug and fines particles. It is proposed that larger agglomerates may be subjected to greater deagglomeration forces during aerosolisation than smaller agglomerates, thus producing an increase in formulation performance. The mechanism underlying the improved performance of ternary formulations where the drug was more cohesive than adhesive to the fines was unclear, but it is possible that this may be attributable to an increased number of particle–particle collisions during the aerosolisation of these formulations.

The mechanism(s) by which fines are effective may depend upon formulation components, proportions, processing and aerosolisation conditions, so these findings cannot necessarily be extrapolated to other systems. In particular, the use of an inhaler device with greater deagglomeration potential than the *Rotahaler*® (which has one of the lowest resistances of commercially available inhalers (29)) might lead to very different conclusions. It should be noted, however, that the formulations, processing and aerosolisation conditions used in this study are very similar to many of those used in previous work (1).

Further research is necessary, both to verify the proposed agglomerates mechanism and to investigate the mechanism responsible for improving the performance of ternary DPI formulations with a cohesive drug–fines CAB ratio.

ACKNOWLEDGEMENTS

The authors gratefully acknowledge the Engineering and Physical Sciences Research Council and GlaxoSmithKline for their generous funding of this work. The authors gratefully acknowledge the assistance of Andy Smith (Sympatec Ltd.) in obtaining the aerosol cloud particle size distribution data.

REFERENCES

1. M. D. Jones and R. Price. The influence of fine excipient particles on the performance of carrier-based dry powder inhalation formulations. *Pharm. Res.* **23**:1665–1674 (2006).
2. X. M. Zeng, G. P. Martin, S. K. Tee, A. Abu Ghoush, and C. Marriott. Effects of particle size and adding sequence of fine lactose on the deposition of salbutamol sulphate from a dry powder formulation. *Int. J. Pharm.* **182**:133–144 (1999).
3. N. Islam, P. Stewart, I. Larson, and P. Hartley. Lactose surface modification by decantation: are drug–fine lactose ratios the key to better dispersion of salmeterol xinafoate from lactose-interactive mixtures? *Pharm. Res.* **21**:492–499 (2004).
4. H. Adi, P. Stewart, and I. Larson. Influence of different sugars on the dispersion of salmeterol xinafoate in dry powder inhalation formulations. Formula IV: Frontiers in Formulation Science. Royal Society of Chemistry, King's College, London, pp. O23 (2005).
5. H. Adi, I. Larson, and P. J. Stewart. Adhesion and redistribution of salmeterol xinafoate particles in sugar-based mixtures for inhalation. *Int. J. Pharm.* **337**:229–238 (2007).
6. P. Lucas, K. Anderson, and J. N. Staniforth. Protein deposition from dry powder inhalers: fine particle multiplets as performance modifiers. *Pharm. Res.* **15**:562–569 (1998).
7. H. Adi, I. Larson, H. Chiou, P. M. Young, D. Traini, and P. Stewart. Agglomerate strength and dispersion of salmeterol xinafoate from powder mixtures for inhalation. *Pharm. Res.* **23**:2556–2565 (2006).
8. X. M. Zeng, G. P. Martin, C. Marriott, and J. Pritchard. Lactose as a carrier in dry powder formulations: the influence of surface characteristics on drug delivery. *J. Pharm. Sci.* **90**:1424–1434 (2001).
9. X. M. Zeng, K. H. Pandhal, and G. P. Martin. The influence of lactose carrier on the content homogeneity and dispersibility of beclomethasone dipropionate from dry powder aerosols. *Int. J. Pharm.* **197**:41–52 (2000).
10. M. D. Louey and P. J. Stewart. Particle interactions involved in aerosol dispersion of ternary interactive mixtures. *Pharm. Res.* **19**:1524–1531 (2002).
11. P. Begat, D. A. V. Morton, J. N. Staniforth, and R. Price. The cohesive–adhesive balances in dry powder inhaler formulations I: direct quantification by atomic force microscopy. *Pharm. Res.* **21**:1591–1597 (2004).
12. M. Bunker, M. Davies, and C. Roberts. Towards screening of inhalation formulations: measuring interactions with atomic force microscopy. *Expert Opin. Drug Del.* **2**:613–624 (2005).
13. P. Begat, D. A. V. Morton, J. N. Staniforth, and R. Price. The cohesive–adhesive balances in dry powder inhaler formulations II: influence on fine particle delivery characteristics. *Pharm. Res.* **21**:1826–1833 (2004).
14. P. Begat, R. Price, H. Harris, D. A. V. Morton, and J. N. Staniforth. The influence of force control agents on the cohesive–adhesive balance in dry powder inhaler formulations. *KONA* **23**:109–121 (2005).
15. J. C. Hooton, M. D. Jones, and R. Price. Predicting the behavior of novel sugar carriers for dry powder inhaler formulations via the use of a cohesive–adhesive force balance approach. *J. Pharm. Sci.* **95**:1288–1297 (2006).
16. D. El-Sabawi, R. Price, S. Edge, and P. M. Young. Novel temperature controlled surface dissolution of excipient particles for carrier based dry powder inhaler formulation. *Drug Dev. Ind. Pharm.* **32**:243–251 (2006).
17. F. R. Fronczek, H. N. Kamel, and M. Slattery. Three polymorphs (α, β and δ) of D-mannitol at 100 K. *Acta Crystallogr., C Cryst. Struct. Commun.* **59**:567–570 (2003).
18. J. Albertsson, A. Oskarsson, and C. Svensson. X-ray study of budesonide: molecular structures and solid solutions of the (22S) and (22R) epimers of 11β,21-dihydroxy-16α,17α-propylmethylenedioxy-1,4-pregnadiene-3,20-dione. *Acta Crystallogr., B Struct. Sci.* **34**:3027–3036 (1978).
19. K. Jarring, T. Larsson, B. Stensland, and I. Ymen. Thermodynamic stability and crystal structures for polymorphs and solvates of formoterol fumarate. *J. Pharm. Sci.* **95**:1144–1161 (2006).
20. B. Y. Shekunov, J. C. Feeley, A. H. L. Chow, H. H. Y. Tong, and P. York. Physical properties of supercritically-processed and micronised powders for respiratory drug delivery. *KONA* **20**:178–187 (2002).
21. G. M. Brown, D. C. Rohrer, B. Berking, C. A. Beevers, R. O. Gould, and R. Simpson. The crystal structure of α,α-trehalose

dihydrate from three independent X-ray determinations. *Acta Crystallogr., B Struct. Sci.* **28**:3145–3158 (1972).
22. S. L. Raghavan, R. I. Ristic, D. B. Sheen, J. N. Sherwood, L. Trowbridge, and P. York. Morphology of crystals of α-lactose hydrate grown from aqueous solution. *J. Phys. Chem. B* **104**:12256–12262 (2000).
23. C. Ceccarelli, G. A. Jeffrey, and R. K. McMullan. A neutron-diffraction refinement of the crystal structure of erythritol at 22.6 K. *Acta Crystallogr. B Struct. Sci.* **36**:3079–3083 (1980).
24. GlaxoSmithKline. Crystal structure of fluticasone propionate (form 1) (unpublished data).
25. P. M. Young, R. Price, M. J. Tobyn, M. Buttrum, and F. Dey. Investigation into the effect of humidity on drug–drug interactions using the atomic force microscope. *J. Pharm. Sci.* **92**:815–822 (2003).
26. F. E. M. O'Brien. The control of humidity by saturated salt solutions. *J. Sci. Instrum.* **25**:73–76 (1948).
27. V. A. Marple, B. A. Olson, K. Santhanakrishnan, J. P. Mitchell, S. C. Murray, and B. L. Hudson-Curtis. Next generation pharmaceutical impactor (a new impactor for pharmaceutical inhaler testing). Part II: Archival calibration. *J. Aerosol Med.* **16**:301–324 (2003).
28. A. H. de Boer, D. Gjaltema, P. Hagedoorn, M. Schaller, W. Witt, and H. W. Frijlink. Design and application of a new modular adapter for laser diffraction characterization of inhalation aerosols. *Int. J. Pharm*. **249**:233–245 (2002).
29. H. W. Frijlink, and A. H. de Boer. Dry powder inhalers for pulmonary drug delivery. *Expert Opin. Drug Del.* **1**:67–86 (2004).
30. J. C. Hooton, M. D. Jones, and R. Price. The effect of the use of a cohesive drug when predicting performance of dry powder inhalation formulations through the cohesive adhesive balance technique, Proceedings of Drug Delivery to the Lungs 16, The Aerosol Society, Edinburgh, UK, pp. 143–146 (2005).
31. H. Steckel and N. Bolzen. Alternative sugars as potential carriers for dry powder inhalations. *Int. J. Pharm.* **270**:297–306 (2004).
32. T. Hartmann and H. Steckel. Influence of mixer type and mixing conditions on delivery efficiency from Flowcaps, a capsule-based dry powder inhaler, Proceedings of Drug Delivery To The Lungs 15, The Aerosol Society, London, UK, pp. 178–181 (2004).
33. J. D. Lord and J. N. Staniforth. Particle size effects on packing and dispersion of powders. In R. N. Dalby, P. R. Byron, and S. J. Farr (eds.), *Respiratory Drug Delivery V* (R. N. Dalby, P. R. Byron, and S. J. Farr, eds). Interpharm Press Inc., pp. 75–84 (1996).
34. A. H. Ibrahim, P. F. Dunn, and R. M. Brach. Microparticle detachment from surfaces exposed to turbulent air flow: controlled experiments and modeling. *J. Aerosol. Sci.* **34**:765–782 (2003).
35. D. A. Braaten, K. T. Paw, and R. H. Shaw. Particle resuspension in a turbulent boundary—layer observed and modeled. *J. Aerosol. Sci.* **21**:613–628 (1990).
36. C. I. Fairchild and M. I. Tillery. Wind-tunnel measurements of the resuspension of ideal particles. *Atmos. Environ.* **16**:229–238 (1982).
37. A. H. Ibrahim, P. F. Dunn, and R. M. Brach. Microparticle detachment from surfaces exposed to turbulent air flow: effects of flow and particle deposition characteristics. *J. Aerosol. Sci.* **35**:805–821 (2004).
38. W. John. Particle–surface interactions: charge transfer, energy loss, resuspension, and deagglomeration. *Aerosol Sci. Technol.* **23**:2–24 (1995).
39. W. John, D. N. Fritter, and W. Winklmayr. Resuspension induced by impacting particles. *J. Aerosol. Sci.* **22**:723–736 (1991).
40. W. John and V. Sethi. Threshold for resuspension by particle impaction. *Aerosol Sci. Technol.* **19**:69–79 (1993).
41. W. Theerachaisupakij, S. Matsusaka, Y. Akashi, and H. Masuda. Reentrainment of deposited particles by drag and aerosol collision. *J. Aerosol. Sci.* **34**:261–274 (2003).
42. J. P. Mitchell and M. W. Nagel. Particle size analysis of aerosols from medicinal inhalers. *KONA* **22**:32–65 (2004).